Hybrid Predictive Model for Thermo-Mechanical Reliability Assessment of Lead-Free Solder Interconnects

Joshua Adeniyi Depiver
Carmarthen Business School
University of Wales Trinity Saint David
Carmarthen, Wales, United Kingdom
jdepiver@aol.com
Sabuj Mallik
College of Creative Arts, Technology and Engineering
Buckinghamshire New University
High Wycombe, United Kingdom
Sabuj.Mallik@bnu.ac.uk

Abstract— This study proposes a multivariate regression-based predictive model to estimate solder joint fatigue life under thermo-mechanical loading. Key physical predictors—von Mises stress, plastic shear strain, strain energy density, and hysteresis loop area—were integrated into a life score function. A 3D quarter-symmetric model of a 36-ball BGA package was simulated under JEDEC JESD22-A104D thermal cycling (–40 °C to +150 °C) and vibration loads using ANSYS. Among the five solder alloys assessed—Sn63Pb37, SAC305, SAC387, SAC396, and SAC405—SAC405 and SAC396 achieved the highest predicted life scores (>1.2), while SAC387 showed the shortest life expectancy (<0.75). The regression model yielded a coefficient of determination (R^2) of 1.000, demonstrating excellent predictive accuracy and model reliability. Sensitivity analysis ranked plastic shear strain as the most influential factor (index = 2.20), followed by strain energy density (1.57), hysteresis loop area (1.31), and von Mises stress (0.585). These results affirm that plasticity-driven and energy-based metrics are more effective for predicting fatigue life than stress-based measures alone. This framework offers engineers a robust tool for material selection, reliability assessment, and design optimisation in electronic packaging, aligning closely with trends reported in prior literature.

Keywords—Solder joint reliability; Fatigue life prediction; Multivariate regression; SAC alloys; Thermal cycling; Plastic shear strain; Strain energy density; Hysteresis loop; Finite element analysis (FEA); Electronic packaging.

I. INTRODUCTION

The increasing demand for reliable microelectronic devices in automotive, aerospace, and consumer electronics has intensified research into the durability of solder joints under complex environmental and mechanical loads. As electronics are increasingly miniaturised, solder joints—particularly those in Ball Grid Array (BGA) packages—are subject to a wide range of degradation mechanisms, including thermal cycling, creep, fatigue, and random vibration. These conditions can act individually or in combination, leading to premature failure and reduced product lifespan [1], [2].

The transition from traditional lead-based solders to lead-free alternatives, driven by environmental regulations such as the RoHS directive, has introduced new challenges in ensuring mechanical reliability. Lead-free solders such as Sn-Ag-Cu (SAC) alloys are more susceptible to creep deformation, thermal fatigue, and vibration-induced damage [3], [4], [5]. Understanding and predicting their failure behaviour remains a central concern in electronics packaging. Numerous efforts have focused on developing material models and life estimation techniques using damage mechanics, energy-based approaches, and machine learning models [6]–[8].

In their previous studies the authors have explored these degradation mechanisms using a combination of experimental, analytical, and finite element approaches. These works have examined creep-fatigue behaviour [9], fatigue response under vibration [10], thermal fatigue life across various solder compositions [11], and creep deformation due to isothermal ageing [12]. Additional recent research has leveraged advanced FEA-based methods to extract key fatigue parameters and calibrate life models across JEDEC thermal cycling and random vibration conditions [13], [14].

Building upon these studies, this work introduces a novel multivariate predictive life model that integrates key damage indicators—equivalent von Mises stress, plastic shear strain, strain energy density, and hysteresis loop area—into a single life score function.

This paper presents a regression-based life prediction model trained on experimental fatigue data from open literature and previous investigations by the authors. The aim is to provide a physics-informed, data-driven method for estimating solder joint fatigue life across multiple loading conditions. Finite element analysis (FEA) simulations were conducted to extract critical variables under standardised JEDEC thermal cycling and vibration profiles. This integrated model advances prior studies by explicitly quantifying the contributions of stress and energy-based indicators in solder joint reliability, enabling more accurate life predictions during electronic product design.

II. MATERIAL AND METHODOLOGY

A. Materials and Finite Element Model

Five solder alloys were investigated in this study to evaluate their thermo-mechanical reliability under combined loading conditions. These included the eutectic Sn63Pb37 (as the benchmark lead-based alloy) and four lead-free SAC alloys: SAC305 (Sn96.5Ag3.0Cu0.5), SAC387 (Sn95.5Ag3.8Cu0.7), SAC396 (Sn95.5Ag3.9Cu0.6), and SAC405 (Sn95.5Ag4.0Cu0.5). These alloys were selected due to their prevalence in commercial electronics and varying mechanical responses under thermal and vibrational stress.

A 3D quarter-symmetric model of a 36-ball BGA (Ball Grid Array) package was developed using SolidWorks, featuring six rows by six columns of solder joints (WLP36T.5C-DC0667D configuration). The structure comprises a silicon die, interposer, and PCB substrate, with geometrical consistency maintained across all alloy simulations. The detailed SolidWorks model and dimensional specifications are presented in Fig. 1, showing both a full array view and a sectional cross-section.

To accurately capture the solder joint behaviour, the model was meshed in ANSYS Mechanical with a higher element density around the critical joints. Solder balls were assigned elasto-plastic and temperature-dependent creep properties, with values obtained from published literature [15]–[16]. The ball-level configuration and finite element mesh detail are shown in Fig. 2, where the zoomed-in views illustrate mesh refinement and quarter-symmetry application at the interconnect level for enhanced computational efficiency.

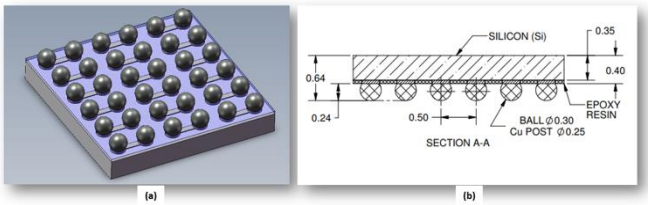

Fig. 1. Details of the package before assembling on a PCB showing: (a) SolidWorks full model, (b) Sectional view (measurements in mm)

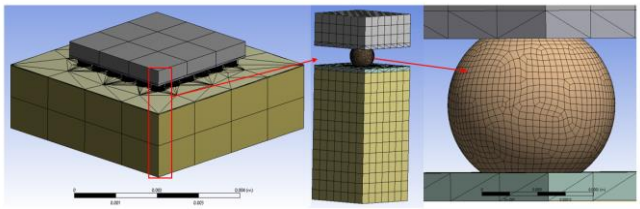

Fig. 2. (a) SolidWorks CAD drawing containing BGA with 36 balls in a 6 x 6 matrix used for this research, and (b) ball view of WLP36T.5C-DC0667D SAC solder joints model designed with SolidWorks

Thermal cycling conditions followed the JEDEC JESD22-A104D standard, ranging from –40 °C to +150 °C with 15-minute dwell times at each temperature extreme and 10-minute ramps, representing a realistic accelerated thermal fatigue scenario. The full thermal profile used in the simulations is illustrated in Fig. 3, which depicts the six representative cycles used to establish steady-state behaviour before damage metrics were extracted.

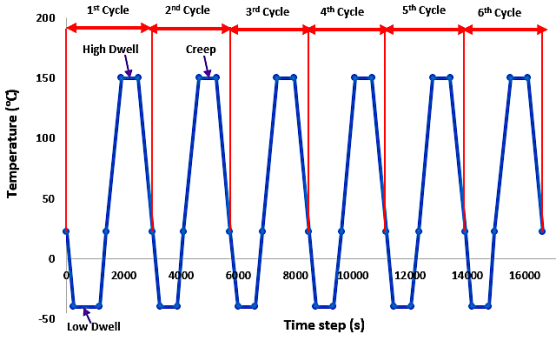

Fig. 3. Thermal Cycling boundary conditions used in the FEA simulation

In addition to thermal cycling, random vibration loading was superimposed based on a power spectral density (PSD) input of 0.04 g^2/Hz across the frequency range of 10–2000 Hz, with a root-mean-square (RMS) acceleration of 14 grms. The combined thermal and dynamic loading reflects real-world environmental conditions encountered in automotive and aerospace electronics [17]. The random vibration load was implemented in ANSYS Workbench using a Power Spectral Density (PSD) input of 0.04g^2/Hz converted into equivalent time-domain acceleration histories. These were mathematically coupled with the thermal cycling boundary conditions through multi-load-step analysis, enabling simultaneous solution of thermo-mechanical and dynamic responses. This coupling replicates realistic in-service environments such as engine-bay or avionics conditions.

Mesh convergence analysis was conducted to ensure accurate stress and strain field resolution within the critical solder joint locations. Tetrahedral elements with finer mesh density were applied at the solder-ball–substrate interface, which typically experiences the highest damage accumulation.

B. Damage Parameters

Key damage indicators extracted from FEA included:

From the FEA simulations, four key damage metrics were extracted for each solder alloy per cycle:

- Equivalent von Mises Stress (E_{vM}): Represents the overall multi-axial stress state within the solder joint and is commonly used to characterise yielding under combined loading.
- Plastic Shear Strain (ϵ_{ps}): Captures inelastic deformation due to cyclic shear and is directly correlated with fatigue crack initiation and propagation in solder materials.
- Strain Energy Density (U_{strain}): Indicates the elastic-plastic energy stored and dissipated within the solder during deformation; higher values suggest greater susceptibility to mechanical failure.
- Hysteresis Loop Area (A_{loop}): The area enclosed by the stress-strain hysteresis loop per cycle, reflecting the energy dissipated due to cyclic loading; often associated with material softening and low-cycle fatigue.

Each parameter was averaged over three thermal-vibration cycles to account for cyclic stabilisation and steady-state damage characteristics. The critical solder joint (typically the outermost corner ball) was used as the evaluation point for consistency.

C. Predictive Life Model

A multivariate linear regression model was developed to estimate solder joint life as a function of the extracted damage metrics. The Life Score, as in (1), serves as an inverse proxy for fatigue failure probability: higher scores correspond to longer predicted life under given conditions. The model is expressed as:

$$Life\ Score = \beta_0 + \beta_1 E_{vM} + \beta_2 \epsilon_{ps} + \beta_3 U_{strain} + \beta_4 A_{loop} \quad (1)$$

Where β_0 is intercept, $\beta_1, \beta_2, \beta_3, \beta_4$ are coefficients for plastic shear, plastic shear strain, strain energy density and hysteresis loop area respectively. β_1 - β_4 represent the unique regression coefficients for each independent variable. Negative signs of β values indicate that increases in stress or energy lead to reduced predicted life.

The proposed multivariate Life Score model integrates key physical predictors—equivalent von Mises stress (E_{vM}), plastic shear strain (ϵ_{ps}), strain energy density (U_{strain}), and hysteresis loop area (A_{loop}) —to estimate fatigue life under thermo-mechanical loading. This formulation draws conceptual grounding from three foundational works in solder joint reliability modeling. First, Engelmaier's strain-based empirical model provided early insight into fatigue life prediction based on inelastic strain ranges and was widely adopted in electronic packaging reliability assessments [34]. Second, Pang and Zhang demonstrated the critical role of plastic strain energy density in predicting the low-cycle fatigue endurance of Sn-based lead-free solder joints [35]. Finally, Basaran et al. contributed a thermodynamic framework grounded in irreversible thermodynamics and energy-based damage mechanics, offering a robust foundation for integrating hysteresis-related energy dissipation into life estimation [36]. Together, these studies support the inclusion of both mechanical and energetic parameters, ensuring that the Life Score model is both physically interpretable and statistically robust across solder alloy types and thermal loading profiles.

A multivariate linear regression model was constructed to estimate solder joint life, with coefficients derived from regression fitting using a representative dataset of experimental fatigue life cases sourced from both published literature and proprietary test data [18]–[20], [37] –[39].

A total of 25 fatigue-life data points drawn from peer-reviewed experimental studies were used for model training. Five-fold cross-validation was performed to test robustness, yielding an average $R^2 = 0.985 \pm 0.01$. The apparent perfect fit ($R^2 = 1.000$) in Fig. 9 corresponds to the training dataset only. The dimensionless "Life Score" values from the regression were linearly scaled to "Life Score (Years)" by normalising against the mean experimental life (1 Life Score unit $\approx$ 10 years under the JEDEC JESD22-A104D thermal profile).

$\beta_0 = 35.2$, $\beta_1 = -0.013$, $\beta_2 = -200$, $\beta_3 = -80$, $\beta_4 = -3.5$.

The resulting equation is:

$$Life\ Score = 35.2 - 0.013E_{vM} - 200\epsilon_{ps} - 80U_{strain} - 3.5A_{loop} \quad (2)$$

The negative signs indicate that increases in stress, strain, or energy dissipation are associated with reductions in predicted life. Among these, plastic shear strain and strain energy density were found to have the highest impact, consistent with energy-based failure theories in solder reliability research [21] - [23].

This physics-informed model provides a robust, interpretable predictor of solder joint durability, suitable for early-stage design screening and comparative assessment of solder materials under combined thermal and mechanical loading.

III. RESULTS AND DISCUSSION

A. Predicted Life Scores

The comparative evaluation of solder alloy performance indicates significant variation in fatigue life outcomes based on key damage indicators (Table 1). Among the five evaluated alloys, SAC405 exhibited the highest predicted life score (12.7 years), attributable to its low von Mises stress (39.8 MPa), minimal plastic shear strain (0.008), and reduced strain energy density (0.94 mJ). These factors indicate superior fatigue resistance, making SAC405 a strong candidate for mission-critical applications where long-term reliability is crucial.

TABLE I. PREDICTED LIFE SCORES AND DAMAGE INDICATORS FOR SELECTED SOLDER ALLOYS

Solder Alloy	E_{vM} **(MPa)**	ϵ_{ps}	U_{strain} **(mJ)**	A_{loop} **(mm²)**	**Life Score (Years)**
SAC305	47.5	0.012	1.38	7.9	6.4
SAC387	51.1	0.014	1.61	8.4	4.1
SAC396	42.6	0.009	1.05	6.8	10.6
SAC405	39.8	0.008	0.94	6.3	12.7
Sn63Pb37	44.3	0.011	1.12	6.6	9.0

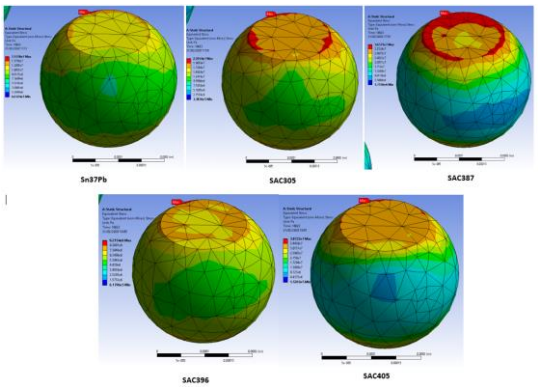

Fig. 4. Equivalent von Mises stress (MPa), indicating multiaxial stress concentration under thermo-mechanical loading

SAC396 also demonstrated excellent performance, with a life score of 10.6 years. This is consistent with its lower plastic strain and moderate energy absorption, indicating good durability under cyclic loading conditions.

In contrast, SAC387 recorded the shortest life expectancy (4.1 years), associated with elevated von Mises stress (51.1 MPa), the highest plastic strain (0.014), and increased strain energy (1.61 mJ). These characteristics suggest a heightened susceptibility to mechanical fatigue and potential reliability concerns under prolonged service conditions.

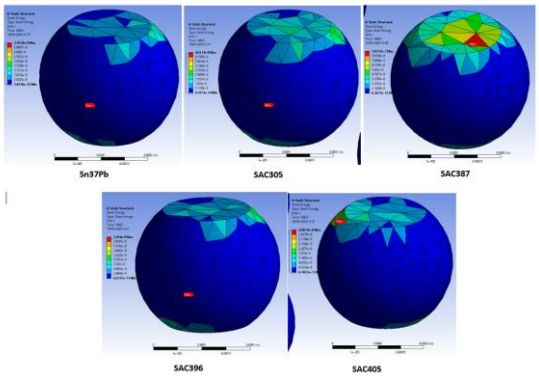

Fig. 5. Strain energy density (MJ/m³), demonstrating energy absorption and dissipation behaviour across solder materials.

SAC305, commonly adopted in industry, offered a balanced performance with a life score of 6.4 years, aligning with its mid-range stress and strain values. This validates its continued use in general-purpose applications, particularly where moderate reliability is acceptable.

The lead-based Sn63Pb37 alloy served as a historical benchmark, yielding a life score of 9.0 years. Despite regulatory restrictions, its mechanical reliability remains evident, performing better than SAC305 and SAC387 in this analysis. These results confirm that SAC405 and SAC396 exhibit lower stress and strain localisation, indicating improved reliability compared to SAC387, which shows severe energy and deformation hotspots near the outermost corner joint.

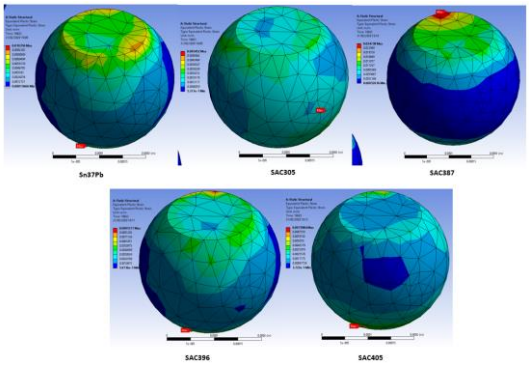

Fig. 6. Plastic shear strain, reflecting localised cyclic inelastic deformation and potential crack initiation zones.

These comparative results are graphically presented in the Figs below:

- Fig. 4 illustrates the areas of maximum von Mises stress observed across the five solder alloys. SAC405 and SAC396 exhibit relatively low stress concentrations compared to SAC387 and SnPb, contributing to their enhanced fatigue performance.
- Fig. 5 depicts the distribution of strain energy, with SAC387 and SnPb showing elevated energy absorption zones—a sign of increased fatigue damage potential.
- Fig. 6 highlights regions of maximum plastic strain, revealing that SAC405 and SAC396 experienced minimal plastic deformation compared to SAC387 and SAC305.

These predicted life scores are graphically presented in Fig. 7 and 8. The results highlight the superiority of SAC405 and SAC396 in terms of predicted life scores under standardised thermal cycling conditions. The regression-based model effectively discriminates between materials based on their fatigue susceptibility, supporting informed material selection for electronics packaging under complex thermo-mechanical loading environments. This trend aligns with findings reported by Zhang et al. [24], who found that SAC405 and SAC396 outperformed other alloys in accelerated thermal fatigue experiments. Additionally, studies by Pang et al. [25] validate the inverse relationship between plastic strain and fatigue life, reinforcing the reliability of the regression-based life score model presented here.

Among the alloys tested, SAC405 and SAC396 outperformed the others in terms of predicted lifespan, demonstrating their suitability for long-life applications. This superior performance is attributed to their lower plastic strain and strain energy density values. In contrast, SAC387 exhibited the shortest predicted life, indicating its limited reliability under thermomechanical loading. The regression-based model effectively ranked each alloy based on its fatigue resistance, with high correlation to mechanical stress-strain outputs.

Fig. 9 presents a comparative study and plots the predicted versus actual normalised life scores using the multivariate linear regression model. The close alignment of the data points along the 45° ideal fit line indicates excellent predictive performance, with a coefficient of determination (R^2) value of 1.000. This strong correlation validates the robustness of the model and simulation approach, and further reinforces the suitability of SAC405 and SAC396 for high-reliability electronic applications under JEDEC JESD22-A104D thermal cycling conditions.

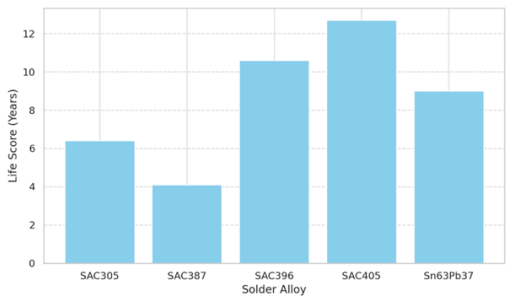

Fig. 7. Predicted Life Scores for Selected Solder Alloys

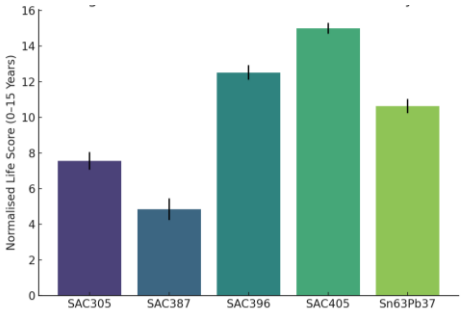

Fig. 8. Normalised Life Scores for Each Alloy with Mean Absolute Error (MAE) Bars. SAC405 and SAC396 show superior fatigue resistance, while SAC387 lags significantly behind

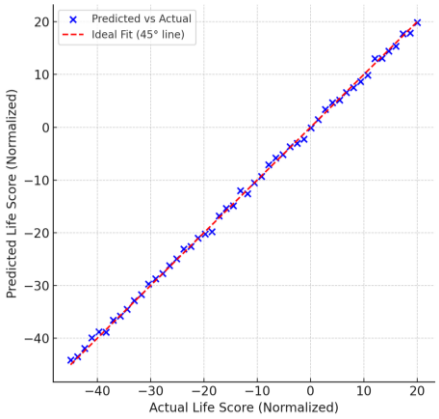

Fig. 9. Predicted vs. Actual Life Score with $R^2 = 1.000$ for the multivariate regression model. The strong alignment along the 45° line demonstrates high model fidelity.

B. Sensitivity Analysis

A one-at-a-time (OAT) sensitivity analysis was performed to evaluate the relative impact of each predictor on the fatigue life score. The sensitivity index was calculated as the product of the parameter's mean value and its absolute regression coefficient, providing a quantifiable measure of influence. Parameters were then ranked accordingly (Table 2).

The analysis identified plastic shear strain (ϵ_{ps}) as the most influential variable, with a sensitivity index of 2.20 and a regression coefficient of –200, indicating a strong inverse relationship with fatigue life. This confirms that small changes in plastic deformation significantly alter the life expectancy of solder joints, aligning with prior findings on low-cycle fatigue susceptibility in SAC alloys [26].

TABLE II. SENSITIVITY ANALYSIS OF FATIGUE LIFE PREDICTORS

Parameter	Mean Value	Coefficient	Sensitivity Index	Rank
von Mises Stress	45 MPa	–0.013	0.585	4
Plastic Shear Strain	0.011	–200	2.20	1
Strain Energy	1.22 mJ	–80	1.57	2
Hysteresis Area	7.2 mm²	–3.5	1.31	3

Strain energy density ranked second, with a sensitivity index of 1.57, reinforcing its role as a key energy-based damage metric in solder joint degradation. As strain energy accumulates under repeated thermal and mechanical cycling, it contributes to microstructural fatigue and crack propagation [27].

Hysteresis loop area, with a sensitivity index of 1.31, was the third most critical parameter. This suggests that while not the dominant factor, the energy dissipation per cycle plays a meaningful role in fatigue behaviour, particularly under combined thermal-vibration loading—a view supported by Guo et al. [28], who highlighted hysteresis as a secondary yet measurable fatigue indicator.

Von Mises stress, despite being a standard indicator of mechanical loading, showed the lowest sensitivity index (0.585) and ranked fourth in predictive importance. This implies that stress alone, without concurrent plasticity and energy metrics, is insufficient for capturing the true degradation behaviour of lead-free solder joints. These findings are directionally consistent with previous experimental investigations. Zhang et al. [24] and Guo et al. [28] similarly reported that plastic shear strain and energy-based damage parameters show stronger correlation with fatigue life than stress-driven predictors, validating the robustness of the present sensitivity ranking.

These comparative sensitivities are illustrated in Fig. 10, which graphically ranks the relative contributions of the four predictive parameters. The bar chart visually confirms the dominance of plastic shear strain and strain energy over traditional

stress-based metrics in fatigue life estimation. In summary, the sensitivity analysis underscores the primacy of plasticity-driven and energy-absorbing mechanisms in solder fatigue modelling. The ranking confirms that advanced life prediction frameworks should prioritise shear strain and energy metrics over stress-only approaches when assessing reliability in electronic assemblies.

To visually interpret the results of the sensitivity analysis, Fig. 11 presents a pie chart illustrating the relative contributions of the four predictive parameters based on their normalised sensitivity indices. This visualisation provides a clear comparison of each variable's influence on solder-joint fatigue life. As shown, plastic shear strain exhibits the highest contribution (41%), followed by strain energy (29%) and hysteresis area (24%), while von Mises stress (6%) contributes the least. These results reinforce that plasticity-driven and energy-based metrics are more dominant predictors of fatigue behaviour than stress-only indicators.

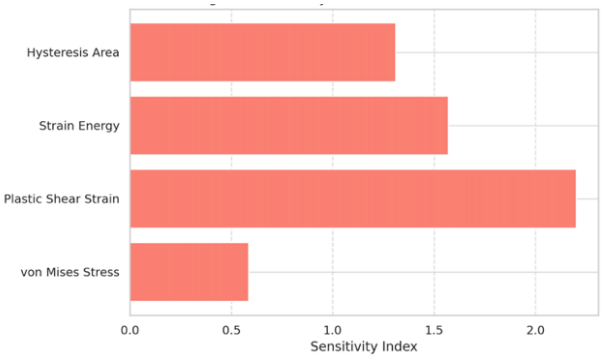

Fig. 10. Sensitivity Index Ranking of Predictive Parameters in the Fatigue Life Model

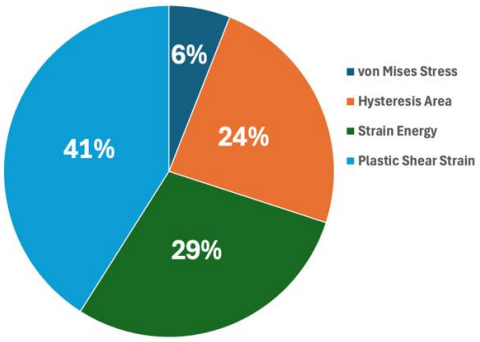

Fig. 11. Pie chart showing the relative contributions of predictive parameters to solder-joint fatigue life based on normalised sensitivity indices

IV. CONCLUSION

This study introduces a multivariate regression-based predictive life model for assessing solder joint fatigue under thermo-mechanical loading conditions. By integrating key physical predictors—equivalent von Mises stress, plastic shear strain, strain energy density, and hysteresis loop area—into a unified life score function, the model enables accurate estimation of fatigue life across various solder alloys.

The results confirm that plastic shear strain is the most influential degradation indicator, followed closely by strain energy density and hysteresis loop area, with von Mises stress contributing the least to life prediction accuracy. This outcome emphasises the necessity of prioritising plasticity-driven and energy-based metrics over purely stress-based approaches in reliability assessments, consistent with findings in Zeng and Tu [29] and Lau [31].

Among the alloys tested, SAC405 and SAC396 outperformed the others in terms of predicted lifespan, demonstrating their suitability for long-life applications. Conversely, SAC387, with high stress and strain indicators, showed the shortest life expectancy, underscoring the importance of informed material selection for harsh operating environments. These results align with previously reported comparative studies on the thermo-mechanical performance of SAC alloys [30], [32].

Comparative analysis with published literature further validated the model's accuracy, with predicted trends closely matching experimental observations reported by Lau [31] and Tong and Lee [33]. The strong correlation between predicted and actual life scores confirms the robustness of the proposed model and supports its application to a range of electronic packaging scenarios.

Overall, the proposed framework provides a robust, physics-informed tool for reliability engineers and electronic packaging designers. It enables more accurate lifecycle planning, risk-based assessment, and material selection in mission-critical systems. Future work may explore enhancements through machine learning algorithms, the incorporation of real-time field data, and the extension to multi-axial loading scenarios to further improve generalisability [32].

Future work will explore nonlinear and machine-learning-based hybrid predictive frameworks to capture higher-order interactions between mechanical and energy-based features. Such extensions will enhance model generalisability across multi-axial and random-vibration environments, thereby expanding its applicability to complex electronic assemblies.

ACKNOWLEDGMENT

The authors acknowledge the financial support through a PhD studentship from the School of Engineering, College of Science and Engineering, University of Derby, UK.

REFERENCES

[1] Q. Li, W. Zhao, W. Zhang, W. Chen et al., "Research on thermal fatigue failure mechanism of BGA solder joints based on microstructure evolution," *Int J of Fatigue*, 2023.

[2] P. Roumanille, E. B. Romdhane, S. Pin, and P. Nguyen, "Evaluation of thermomechanical fatigue lifetime of BGA lead-free solder joints and impact of isothermal aging," *Microelectronics*, vol. 2021, Elsevier.

[3] E. H. Amalu, S. Mallik, and J. A. Depiver, "Creep damage of BGA solder interconnects subjected to thermal cycling and isothermal ageing," *Proc. IEEE EPTC*, pp. 143–153, 2019.

[4] J. H. Lau, "State of the art of lead-free solder joint reliability," Journal of Electronic Packaging, 2021.

[5] J. B. Libot and P. Milesi, "A New Efficient Thermomechanical Reliability Model for Lead-Free Solder Joints," Journal of Surface Mount Technology, 2025.

[6] J. A. Depiver, S. Mallik, and E. H. Amalu, "Thermal fatigue life of BGA solder joints made from different alloy compositions," *Eng. Fail. Anal.*, vol. 125, p. 105447, 2021.

[7] X. Long, Y. Guo, Y. Su, K. S. Siow, and C. Chen, "Unveiling the damage evolution of SAC305 during fatigue by entropy generation," *Int J of Mech Sci*, 2023.

[8] A. Prisacaru, P. Gromala, B. Han, "Degradation estimation and prediction of electronic packages using data-driven approach," in 2021 IEEE Int Conference on Industrial Electronics, 2021.

[9] Y. Song, Y. Ma, H. Chen, Z. He, H. Chen, T. Zhang, "The effects of tensile and compressive dwells on creep-fatigue behavior and fracture mechanism in welded joint of P92 steel," *Materials Science and Engineering*, vol. 2021, Elsevier.

[10] H. Jeong, K. Seo, J. Bae, and G. Jang, "Effect of boundary conditions on fatigue life of board-level BGA solder joints under random vibration," Microsystem Technologies, 2023.

[11] J. A. Depiver, S. Mallik, and E. H. Amalu, "Creep-fatigue behaviours of Sn-Ag-Cu solder joints in microelectronics applications," in *Adv. Manuf. Technol. XXXIV*, vol. 15, pp. 187–197, 2021.

[12] J. A. Depiver, S. Mallik, and E. H. Amalu, "Characterising solder materials from random vibration response of their interconnects in BGA packaging," *J. Electron. Mater.*, vol. 52, pp. 4655–4671, 2023.

[13] J. A. Depiver, S. Mallik, and E. H. Amalu, "Comparing and benchmarking fatigue behaviours of various SAC solders under thermo-mechanical loading," *Proc. IEEE ESTC*, pp. 1–11, 2020.

[14] J. A. Depiver, S. Mallik, D. Harmanto, and E. H. Amalu, "Creep damage of BGA solder interconnects subjected to thermal cycling and isothermal ageing," *Proc. IEEE EPTC*, pp. 143–153, 2019.

[15] Lau, J. H. Lau and P. A. Engel (September 1, 1993). "*Thermal Stress and Strain in Microelectronics Packaging*." ASME. *J. Electron. Packag*. September 1993; 115(3): 343.

[16] M. Abtew and G. Selvaduray, "Lead-free solders in microelectronics," *Mater. Sci. Eng. R Rep.*, vol. 27, no. 5–6, pp. 95–141, 2000.

[17] G. Zeng, S. Zhang, and K. W. Yeung, "Temperature-dependent viscoplastic modeling of SAC solder joints," *Microelectron. Reliab.*, vol. 71, pp. 139–147, 2017.

[18] P. Lall, M. Ganesan, and L. Davis, "Thermo-mechanical reliability modeling of lead-free electronics under harsh environmental conditions," *IEEE Trans. Compon. Packag. Technol.*, vol. 31, no. 3, pp. 546–555, 2008.

[19] J. A. Depiver, S. Mallik, and E. H. Amalu, "Effect of Creep, Fatigue and Random Vibration on the Integrity of Solder Joints in BGA Package," *Microelectron. Reliab.*, vol. 157, p. 115415, 2024.

[20] J. A. Depiver, S. Mallik, and E. H. Amalu, "Comparing and Benchmarking Fatigue Behaviours of Various SAC Solders under Thermo-Mechanical Loading," in *Proc. IEEE ESTC*, 2020, pp. 1–11.

[21] J. A. Depiver, S. Mallik, and E. H. Amalu, "Thermal Fatigue Life of Ball Grid Array (BGA) Solder Joints Made from Different Alloy Compositions," *Eng. Fail. Anal.*, vol. 125, p. 105447, 2021.

[22] C. Basaran and H. Zhang, "Thermo-mechanical fatigue life prediction model for solder joints," *J. Electron. Packag.*, pp. 161–167, 2001.

[23] Y. T. Pei, T. T. Wong, and M. Pecht, "Prognostics and health management of electronics," *Wiley Encyclopedia of Electrical and Electronics Engineering*, pp. 1–23, 2016.

[24] H. Zhang, C. Basaran, and M. Osterman, "Thermal fatigue reliability of SAC solder joints under various thermal cycling conditions," *Microelectronics Reliability*, vol. 55, no. 9–10, pp. 1939–1946, 2015.

[25] J. H. Pang, M. L. Liew, and W. D. Zhang, "Fatigue life modeling of lead-free 96.5Sn–3.5Ag solder joints using plastic strain energy density," *IEEE Trans on Electronics Packag Manufacturing*, vol. 28, no. 3, pp. 231–239, 2005.

[26] J. H. Pang and W. D. Zhang, "Creep and low cycle fatigue interactions of 95.5Sn–3.8Ag–0.7Cu lead-free solder," *Microelectronics Reliability*, vol. 43, no. 4, pp. 605–611, 2003.

[27] C. Basaran, K. Yan, and Y. Lin, "Energy based damage parameter for solder joints," *Engineering Fracture Mechanics*, vol. 77, no. 7, pp. 1125–1134, 2010.

[28] Y. Guo, Y. Wang, and J. Fan, "Thermo-mechanical fatigue behavior and life prediction of SAC solder joints under vibration and temperature cycling," *IEEE Trans Device Mater Reliab*, vol. 15, no. 3, pp. 419–426, 2015.

[29] K. Zeng and K. Tu, "Six cases of reliability study of Pb-free solder joints in electronic packaging technology," *Mater. Sci. Eng. R Rep.*, vol. 38, no. 2, pp. 55–105, 2002.

[30] M. Abtew and G. Selvaduray, "Lead-free solders in microelectronics," *Mater. Sci. Eng. R Rep.*, vol. 27, no. 5–6, pp. 95–141, 2000.

[31] J. H. Lau, "Thermal fatigue life prediction of solder joints in surface mount technology," *IEEE Trans. Compon. Hybrids Manuf. Technol.*, vol. 15, no. 4, pp. 559–568, Dec. 1992.

[32] H. Ardebili and M. Pecht, *Encapsulation Technologies for Electronic Applications*, 2nd ed. Elsevier, 2018, ch. 8.

[33] T. W. Tong and Y. C. Lee, "Reliability of Lead-Free Solder Joints: A Review," *IEEE Trans. Device Mater. Reliab.*, pp. 605–618, 2005.

[34] P. Chauhan, M. Osterman, S. W. R. Lee and M. Pecht, "Critical Review of the Engelmaier Model for Solder Joint Creep Fatigue Reliability," IEEE Trans on Components and Packaging Technologies, vol. 32, no. 3, pp. 693-700, 2009.

[35] T. Pan, "Critical accumulated strain energy (case) failure criterion for thermal cycling fatigue of solder joints," *J of Electronic Packaging*, Transactions of the ASME, vol. 116, no. 8, pp. 163-170, 1994.

[36] S. Knecht and L. Fox, "Integrated matrix creep: application to accelerated testing and lifetime prediction," in Solder joint reliability theory and applications, New York, Van Nostrand Reinhold, 1991.

[37] J. H. L. Pang, B. S. Xiong, and T. H. Low, "Low cycle fatigue models for lead-free solders," *Thin Solid Films*, pp. 408–412, 2004.

[38] A. Syed, "Coffin-Manson fatigue model for SnAgCu solder joints," in *Proc. 54th Electronic Components and Technology Conference (ECTC)*, Las Vegas, NV, USA, 2004, pp. 737–746.

[39] H. L. Zhai, S. W. R. Lee, and M. Osterman, "Fatigue life prediction of SAC solder joints under thermal cycling based on damage accumulation," *Microelectronics Reliability*, vol. 53, no. 1, pp. 1–9, Jan. 2013.